Supplement of Atmos. Chem. Phys., 25, 13221–13243, 2025 https://doi.org/10.5194/acp-25-13221-2025-supplement © Author(s) 2025. CC BY 4.0 License.





Supplement of

Contributions of primary anthropogenic sources and rapid secondary transformations to organic aerosol pollution in Nanchang, Central China

Wei Guo et al.

Correspondence to: Huayun Xiao (xiaohuayun@sjtu.edu.cn)

The copyright of individual parts of the supplement might differ from the article licence.

28	This file contains S1 and S2, Table S1 and Table S2, Figure S1 to Figure S12. The detailed
29	information is as follows:
30	1. S1. Meteorological conditions and air qualityPage 1
31	2. S2. Instrumentation and analytical procedures
32	3. Table S1. Details of polar organic compounds identified using the GC/MS methodPage 4–6
33	4. Table S2. Representative compounds from various emission sources and their mass fractions in
34	SOC and SOAPage 7
35	5. Figure S1. Trends of annual PM _{2.5} concentrations from 2013 to 2023 in China and Nanchang (a);
36	variations in daily PM _{2.5} concentrations during the winter of 2023 to 2024 in Nanchang (b); winter
37	PM _{2.5} concentrations in major cities across China in 2023–2024 (c)Page 9
38	6. Figure S2. Time series of meteorological parameters and gaseous pollutant concentrations
39	during sampling periods
40	7. Figure S3. Source profile information used in the CMB model
41	8. Figure S4. The concentration ratios and its seasonal variations of the major polar
42	compoundsPage 13
43	9. Figure S5. Correlation between levoglucosan and some primary sugars, sugar alcohols, lignin,
44	resin products, and sterols (a); correlation between glycerol and hydroxy acids (b)Page 14
45	10. Figure S6. The concentration ratios and its seasonal variations of the SOA tracersPage 15
46	11. Figure S7. Concentrations and relative abundances of primary organic carbon (POC) from
47	biomass burning, coal combustion, vehicle exhaust, cooking, plant debris, and fungal spores, as
48	well as secondary organic carbon (SOC) from isoprene, α/β -pinene, β -caryophyllene, toluene, and
49	naphthalene
50	12. Figure S8. Variations in concentrations and relative abundances of other POC and SOC across
51	different seasons and pollution episodes
52	13. Figure S9. Concentrations and relative abundances of primary organic aerosol (POA) from
53	biomass burning, coal combustion, vehicle exhaust, cooking, plant debris, and fungal spores, as
54	well as secondary organic aerosol (SOA) from isoprene, α/β -pinene, β -caryophyllene, toluene, and
55	naphthalenePage 18
56	14. Figure S10. Time series of POC and SOC concentrations calculated using the tracer-based

57	method, alongside POC and SOC concentrations derived from the EC-based method, as well as
58	PM _{2.5} and measured OC concentrations during the sampling periods
59	15. Figure S11. Time series of POC and SOC concentrations calculated using the tracer-based
60	method, alongside POC and SOC concentrations derived from the EC-based method, as well as
61	PM _{2.5} and measured OC concentrations during winter pollution episodesPage 20
62	16. Figure S12. Linear correlation between wind speed (WS), relative humidity (RH), and SOC
63	for the annual sampling periods (a), winter pollution periods (b), winter remainder (c), and
64	individual winter pollution episodes (d–l)Page 21
65	
66	
67	
68	
69	
70	
71	
72	
73	
74	
75	
76	
77	
78	
79	
80	
81	
82	

S1. Meteorological conditions and air quality

83

84

85

86

87

88

89

90

91

92

93

94

95

96

97

98

99

100

101

102

103

104

105

106

107

108

109

110

111

During the sampling period, wind speed ranged from 0.8 to 4.4 m s⁻¹, with notable peaks in July and October. Wind patterns exhibited seasonal variability: southwest and easterly winds dominated in late spring (May) and summer (June – August), while north and north-easterly winds prevailed in other seasons (Figure S1). The annual rainfall was 3708.9 mm, predominantly concentrated in spring and summer. Atmospheric pressure fluctuated between 900-1040 hPa, displaying an inverse relationship with sunshine duration (10–14 hours). Specifically, pressure was lower in spring and summer, higher in autumn and winter, while sunshine hours showed the complementary trend. Temperature and relative humidity (RH) varied widely, ranging from -0.5 to 33.9 $^{\circ}$ C (mean: 19.7 \pm 8.7 $^{\circ}$ C) and 33.9%–95.9% (mean: 72.0 \pm 13.9%), respectively. The CO, O_3 , SO_2 and NO_2 concentrations were 0.42–1.32 mg m⁻³ (0.74 \pm 0.18 mg m⁻³, 7–187 μ g m⁻³ $(86.33 \pm 36.81 \ \mu g \ m^{-3})$, $3-28 \ \mu g \ m^{-3}$ $(7.92 \pm 4.14 \ \mu g \ m^{-3})$, and $6-84 \ \mu g \ m^{-3}(27.68 \pm 15.11 \ \mu g)$ m⁻³), respectively. Seasonal variations were particularly notable for SO₂ and NO₂. These pollutants exhibited higher concentrations during autumn and winter-coinciding with lower temperatures and reduced rainfall—and decreased levels in spring and summer when temperatures and precipitation were elevated. Conversely, O₃ concentrations demonstrated an inverse seasonal pattern.

S2. Instrumentation and analytical procedures

The analytical conditions employed for gas chromatography (GC) were meticulously optimized to ensure precise qualitative and quantitative assessment of target compounds. Samples were introduced in splitless mode with the injector maintained at 280 °C. The temperature program of the GC oven commenced at an initial hold of 50 °C for 2 minutes, followed by a rapid ramp to 120 °C at a rate of 30 °C min⁻¹. Subsequently, the temperature was incrementally raised to 300 °C at a rate of 6 °C min⁻¹, where it was sustained for 16 minutes. This carefully calibrated thermal profile has been extensively detailed in the existing literature (Wang and Kawamura, 2005; Wang et al., 2006; Fu et al., 2008 and 2010), underscoring its efficacy in the separation of diverse organic compounds.

Qualitative analysis of the target compounds was performed by comparing retention times and ion mass spectra of the compounds in the samples against those of a standard series (see Table S1).

For quantification, the average relative response factor (\overline{RRF}) method was employed. The concentration of target compound x (ρ_x) was calculated using the following formula:

where A_x is response value (peak area) of target compound x, A_{IS} is the response value of the

 $\rho_{x} = \frac{A_{x} \times \rho_{is}}{A_{is} \times RRF},$

115

116

117

118

119

120

121

122

123

124

125

126

127

128

129

130

131

132

133

134

135

136

137

138

139

140

internal standard, ρ_{IS} denotes concentration of the internal standard. The average relative response factor (\overline{RRF}) for the target compound is derived from the individual RRF values of authentic standards (refer to Table S1) measured at various concentrations. Since some of the target compounds' standards were difficult to obtain on the market, their RRF could be substituted with those of other standard compounds with similar properties (Fu et al., 2010 and 2014; Ding et al., 2012; Yuan et al., 2018). Specifically, the hentriacontanoic acid and dotriacontanoic acid were quantified using nonacosanoic acid and triacontanoic acid, respectively. The pentacosanol, nonacosanol, hentriacontanol, dotriacontanol were quantified using tricosanol, heptacosanol, heptacosanol, and triacontanol, respectively. The glyceric acid was quantified using glycerol. The 2-methylglyceric acid, cis-2-methy-1,3,4-trihydroxy-1-butene, 3-methyl-2,3,4-trihydroxy-1-butene, trans-2-methyl-1,3,4-trihydroxy-1-butene, 2-methylthreitol, and 2-methylerythritol quantified using erythritol. The 2,3-dihydroxy-4-oxopentanoic acid was quantified using citric acid. The pinic acid and 3-methyl-1,2,3-butanetricarboxylic acid were quantified using pinonic acid. The β-caryophyllinic acid was quantified using octadecanoic acid (Table S1). The limits of detection (LOD) and quantification (LOO) for the target compounds were determined based on signal-to-noise ratios of 3:1 and 10:1, respectively. In this study, the LODs ranged from 0.05 to $0.30~\text{ng}~\mu\text{L}^{-1}$, which correspond to ambient concentrations of $0.03~\text{to}~0.23~\text{ng}~\text{m}^{-3}$, calculated for a typical sampling volume of 1300 m³. Prior to sampling, all filters were subjected to a baking process at 450 °C for 4 hours to eliminate residual organic contaminants. Additionally, all glassware was rinsed with methanol, dichloromethane, and hexane immediately before use to prevent potential contamination. To ensure data integrity, blank experiments and recovery tests were systematically performed during sample analysis. Field blanks were routinely collected at the end of each month and analyzed alongside the filter samples. The results indicated that background contamination was negligible, accounting for less than 3% of the concentrations found in the samples. Recovery rates for all

- target compounds spiked onto pre-combusted blank filters ranged from 82% to 109% (n = 3) and
- were treated as real samples (Table S1). Data presented herein were adjusted for field blanks but
- were not corrected for recoveries.

References in S1 and S2

- 146 Ding, X., Wang, X. M., Gao, B., Fu, X. X., He, Q. F., Zhao, X. Y., Yu, J. Z., and Zheng, M.:
- 147 Tracer-based estimation of secondary organic carbon in the Pearl River Delta, south China, J.
- Geophys. Res-Atmos., 117, https://doi.org/10.1029/2011JD016596, 2012.
- Fu, P. O., Kawamura, K., Okuzawa, K., Aggarwal, S. G., Wang, G., Kanaya, Y., and Wang, Z.:
- 150 Organic molecular compositions and temporal variations of summertime mountain aerosols
- over Mt. Tai, North China Plain, J. Geophys. Res-Atmos., 113,
- 152 https://doi.org/10.1029/2008JD009900, 2008.
- 153 Fu, P. Q., Kawamura, K., Pavuluri, C. M., Swaminathan, T., and Chen, J.: Molecular
- characterization of urban organic aerosol in tropical India: contributions of primary emissions
- and secondary photooxidation, Atmos. Chem. Phys., 10, 2663–2689, https://doi.org/10,
- 156 2663-2689, 10.5194/acp-10-2663-2010, 2010.
- 157 Fu, P. Q., Kawamura, K., Chen, J., and Miyazaki, Y.: Secondary Production of Organic Aerosols
- from Biogenic VOCs over Mt. Fuji, Japan, Environ. Sci. Technol., 48, 8491–8497,
- https://doi.org/10.1021/es500794d, 2014.
- Wang, G. H., and Kawamura, K.: Molecular Characteristics of Urban Organic Aerosols from
- Nanjing: A Case Study of A Mega-City in China, Environ. Sci. Technol., 39, 7430–7438,
- 162 https://doi.org/10.1021/es051055+, 2005.
- Wang, G. H., Kawamura, K., Lee, S., Ho, K., and Cao, J. J.: Molecular, Seasonal, and Spatial
- Distributions of Organic Aerosols from Fourteen Chinese Cities, Environ. Sci. Technol., 40,
- 4619–4625, https://doi.org/10.1021/es060291x, 2006.
- 166 Yuan, Q., Lai, S. C., Song, J. W., Ding, X., Zheng, L. S., Wang, X. M., Zhao, Y., Zheng, J. Y., Yue, D.
- L., Zhong, L.J., Niu, X. J., and Zhang, Y. Y: Seasonal cycles of secondary organic aerosol tracers in
- 168 rural Guangzhou, Southern China: The importance of atmospheric oxidants, Environ. Pollut., 240,
- 169 884–893, https://doi.org/10.1016/j.envpol.2018.05.009, 2018.

170

171172

173

Table S1. Details of polar organic compounds identified using the GC/MS method, including limits of detection (LOD) and quantification (LOQ), selected standards and their concentrations in recovery experiments, along with recovery rates.

Identified compounds	Molecula	m/z	Time	LOD	LOD	LOP	Standard s	Standards	Recovery
rachemea compounds	r formula	III Z	(min)	ng m ⁻³	$\frac{ng}{ul^{-1}}$	ng ul ⁻¹	$ng\ m^{-3}$	CAS	%
Fatty acids									
Decanoic acid	$C_{10}H_{20}O_2$	117, 229	15.8	0.03	0.05	0.12	10	334-48-5	103.94±3
Hendecanoic acid	$C_{11}H_{22}O_2$	117, 243	17.7	0.03	0.05	0.13	10	112-37-8	102.92±2
Lauric acid	$C_{12}H_{24}O_2$	117, 257	19.3	0.06	0.08	0.28	10	143-07-7	94.51 ±2.
Tridecanoic acid	$C_{13}H_{26}O_2$	117, 271	21.3	0.03	0.05	0.14	10	638-53-9	105.59±2
Tetradecanoic acid	$C_{14}H_{28}O_{2} \\$	117, 285	23.5	0.05	0.07	0.23	10	544-63-8	95.66±1
Pentadecylic acid	$C_{15}H_{30}O_2$	117, 299	24.9	0.03	0.05	0.15	10	1002-84-2	98.18±1
Palmitoleic Acid	$C_{16}H_{30}O_2$	117, 313	25.5	0.05	0.06	0.21	10	373-49-9	97.92±0
Palmitic acid	$C_{16}H_{32}O_2$	117, 313	26.5	0.16	0.21	0.71	10	57-10-3	87.47±3
Heptadecanoic acid	$C_{17}H_{34}O_2$	117, 327	28.8	0.12	0.16	0.54	10	506-12-7	94.70±2
Oleic Acid	$C_{18}H_{34}O_2$	117, 341	30.1	0.04	0.06	0.19	10	112-80-1	90.34±5
Octadecanoic acid	$C_{18}H_{36}O_2$	117, 341	30.5	0.10	0.13	0.44	10	57-11-4	93.27 ±2
Nonadecanoic acid	$C_{19}H_{38}O_2$	117, 355	32.4	0.05	0.07	0.22	10	646-30-0	86.48±4
Icosanoic acid	$C_{20}H_{40}O_{2} \\$	117, 369	34.0	0.13	0.17	0.58	10	506-30-9	91.03±0
Henicosanoic acid	$C_{21}H_{42}O_2$	117, 383	35.7	0.13	0.16	0.54	10	2363-71-5	86.84±3
Docosanoic acid	$C_{22}H_{44}O_2$	117, 397	37.3	0.06	0.07	0.24	10	112-85-6	97.33±6
Tricosanoic acid	$C_{23}H_{46}O_2$	117, 411	38.8	0.08	0.11	0.36	10	2433-96-7	108.87±
Tetracosanoic acid	$C_{24}H_{48}O_2$	117, 425	40.3	0.04	0.05	0.16	10	557-59-5	97.39±1
Pentacosanoic acid	$C_{25}H_{50}O_2$	117, 439	41.7	0.12	0.16	0.53	10	506-38-7	88.17±1
Hexacosanoic acid	$C_{26}H_{52}O_2$	117, 453	43.4	0.23	0.30	1.01	10	506-46-7	103.71±
Heptacosanoic acid	$C_{27}H_{54}O_2$	117, 467	44.7	0.04	0.06	0.19	10	7138-40-1	105.24±
Octacosanoic acid	$C_{28}H_{56}O_2$	117, 481	45.5	0.06	0.08	0.27	10	506-48-9	96.44±2
Nonacosanoic acid	$C_{29}H_{58}O_2$	117, 495	46.9	0.07	0.10	0.32	10	4250-38-8	100.22±
Triacontanoic acid	$C_{30}H_{60}O_2$	117, 509	48.2	0.07	0.09	0.29	10	506-50-3	101.73±
Hentriacontanoic acid	$C_{31}H_{62}O_2$	117, 523	50.1	0.05	0.07	0.23	10	4250-38-8 (Nonacosanoic	100.22±
Dotriacontanoic acid	$C_{32}H_{64}O_2$	117, 537	53.8	0.03	0.05	0.15	10	acid) 506-50-3 (Triacontanoic acid)	101.73±
Fatty alcohols									
Tetradecanol	$C_{14}H_{30}O$	75, 271	18.0	0.05	0.07	0.23	10	112-72-1	101.61 ±
Pentadecanol	$C_{15}H_{32}O$	75, 285	20.9	0.04	0.06	0.18	10	629-76-5	108.13±
Hexadecanol	$C_{16}H_{34}O$	75, 299	23.6	0.12	0.16	0.53	10	36653-82-4	90.08±1
Heptadecanol	$C_{17}H_{36}O$	75, 313	26.1	0.03	0.05	0.14	10	1454-85-9	84.56±2
Octadecanol	$\mathrm{C_{18}H_{38}O}$	75, 327	28.4	0.16	0.21	0.71	10	112-92-5	87.61±2
Nonadecanol	$C_{19}H_{40}O$	75, 341	30.1	0.06	0.08	0.27	10	1454-84-8	90.88±0
Eicosanol	$C_{20}H_{42}O$	75, 355	32.3	0.04	0.05	0.17	10	629-96-9	98.27±1
Heneicosanol	$C_{21}H_{44}O$	75, 369	34.5	0.05	0.07	0.23	10	15594-90-8	95.56±2
Docosanol	$C_{22}H_{46}O$	75, 383	36.1	0.04	0.05	0.15	10	661-19-8	108.51±
Tricosanol	$C_{23}H_{48}O$	75, 397	38.6	0.03	0.05	0.13	10	3331-01-5	106.15±
Tetracosanol	$\mathrm{C}_{24}\mathrm{H}_{50}\mathrm{O}$	75, 411	39.1	0.08	0.10	0.34	10	506-51-4	96.03±4
Pentacosanol	$C_{25}H_{52}O$	75, 425	40.5	0.06	0.08	0.27	10	3331-01-5 (Tricosanol)	106.15±
Hexacosanol	$C_{26}H_{54}O$	75, 439	42.3	0.06	0.08	0.25	10	506-52-5	85.91±4

Heptacosanol	$C_{27}H_{56}O$	75, 453	43.5	0.08	0.10	0.33	10	2004-39-9	98.48±4.80
Octacosanol	$C_{28}H_{58}O$	75, 467	45.0	0.10	0.13	0.44	10	557-61-9	92.88±4.34
Nonacosanol	$C_{29}H_{60}O$	75, 481	46.3	0.11	0.15	0.49	10	2004-39-9 (Heptacosanol)	98.48±4.80
Triacontanol	$C_{30}H_{62}O$	75, 495	48.3	0.13	0.17	0.57	10	593-50-0	89.50±3.81
Hentriacontanol	$C_{31}H_{64}O$	75, 509	50.2	0.09	0.11	0.37	n.a.	2004-39-9 (Heptacosanol)	98.48±4.80
Dotriacontanol	$C_{32}H_{66}O$	75, 523	52.7	0.06	0.08	0.27	n.a.	593-50-0 (Triacontanol)	89.50±3.81
Cholesterol	C ₂₇ H ₄₆ O	129, 458	45.1	0.10	0.13	0.45	10	57-88-5	87.23±1.51
Stigmasterol	$C_{29}H_{48}O$	129, 484	46.5	0.08	0.11	0.36	10	83-48-7	98.71±0.85
β-sitosterol	C ₂₉ H ₅₀ O	129, 486	46.8	0.11	0.15	0.49	10	83-46-5	88.32±4.07
Saccharides									
Ribose	$C_5H_{10}O_5$	191, 204, 217	19.5	0.12	0.16	0.53	20	50-69-1	90.34±2.8
Galactosan	$C_6H_{10}O_5$	204, 217, 333	19.8	0.13	0.16	0.55	20	644-76-8	90.29±0.15
Mannosan	$C_6H_{10}O_5$	204, 217, 333	20.1	0.10	0.13	0.44	20	14168-65-1	88.92±2.04
Levoglucosan	$C_6H_{10}O_5$	204, 217, 333	21.2	0.16	0.20	0.68	20	498-07-7	111.28±5.07
Arabitol	$C_5H_{12}O_5$	217, 307, 319	22.3	0.09	0.11	0.37	20	488-82-4	93.33±3.25
Fructose	$C_6H_{12}O_6$	191, 204, 217	22.5	0.09	0.12	0.41	20	57-48-7	89.89±9.50
Pinitol	$C_7H_{14}O_6$	217, 260, 318	22.8	0.06	0.07	0.24	20	10284-63-6	103.43±0.88
Galactose	$C_6H_{12}O_6$	204, 191, 217	23.1	0.07	0.10	0.32	20	59-23-4	88.91±6.66
Glucose	$C_6H_{12}O_6$	191, 204, 217	23.8	0.11	0.15	0.49	20	50-99-7	97.50±2.46
Mannitol	$C_6H_{14}O_6$	205, 217, 319	24.3	0.13	0.16	0.55	20	69-65-8	102.68±3.08
Inositol	$C_6H_{12}O_6$	217, 305, 318	27.1	0.06	0.08	0.27	20	87-89-8	97.82±6.98
Sucrose	$C_{12}H_{22}O_1$	217, 361, 437	35.3	0.05	0.06	0.21	20	57-50-1	93.08±2.96
Lactose	$C_{12}H_{22}O_1$	191, 217, 361	36.2	0.04	0.05	0.16	20	63-42-3	96.02±3.06
Maltose	$C_{12}H_{22}O_1$	204, 217, 361	38.1	0.09	0.11	0.37	20	69-79-4	91.13±4.13
Turanose	$C_{12}H_{22}O_1$	147, 217, 361	38.5	0.07	0.09	0.29	20	547-25-1	94.45±1.10
Trehalose	$C_{12}H_{22}O_1$	147, 217, 361	39.0	0.08	0.10	0.34	20	99-20-7	96.47±6.23
	1								
Others (Monoacids, diacids, polyacids, and polyols)									
Benzoic acid	$C_7H_6O_2$	77, 105, 179	10.5	0.06	0.07	0.24	5	65-85-0	81.66±4.79
Glycerol	$C_3H_8O_3$	73, 171, 308	11.7	0.06	0.08	0.28	5	56-81-5	84.73±1.75
Glyceric acid	$C_3H_6O_4$	73, 247, 292	12.2	0.10	0.13	0.45	5	56-81-5 (Glycerol)	84.73±1.75
2-Methylglyceric acid	$C_4H_8O_4$	203, 219, 306	13.3	0.09	0.11	0.37	5	149-32-6 (Erythritol)	87.19±3.53
Cis-2-methy-1,3,4-trihydroxy-1-butene	$C_5H_{10}O_3$	73, 147, 231	14.2	0.08	0.10	0.33	5	149-32-6 (Erythritol)	87.19±3.53
3-methyl-2,3,4-trihydroxy-1-butene	$C_5H_{10}O_3$	147, 215, 231	15.1	0.10	0.13	0.44	5	149-32-6 (Erythritol)	87.19±3.53
Trans-2-methyl-1,3,4-trihydroxy-1-bute ne	$C_5H_{10}O_3$	73, 147, 231	15.6	0.06	0.07	0.25	5	149-32-6 (Erythritol)	87.19±3.53
Malic acid	$C_4H_6O_5$	73, 245, 287	16.0	0.11	0.15	0.50	5	636-61-3	84.61 ±6.92
2,3-Dihydroxy-4-oxopentanoic acid (DHOPA)	$C_5H_8O_5$	189, 247, 350	16.1	0.10	0.13	0.44	5	77-92-9 (Citric acid)	83.88±1.72
Citric acid	$C_6H_8O_7$	73, 89, 357	16.5	0.19	0.24	0.81	5	77-92-9	83.88±1.72
Pinonic acid	$C_{10}H_{16}O_3$	125, 171, 257	16.8	0.13	0.16	0.54	5	61826-55-9	97.31±6.29
2-Methylthreitol	C ₁₀ H ₁₆ O ₃ C ₅ H ₁₂ O ₄	129, 219, 277	17.8	0.08	0.11	0.35	5	149-32-6 (Erythritol)	87.19±3.53
2-Methylerythritol	$C_5H_{12}O_4$	129, 219, 277	18.0	0.07	0.09	0.30	5	149-32-6 (Erythritol)	87.19±3.53
3-hydroxyglutaric acid	$C_5H_8O_5$	185, 275, 349	18.2	0.09	0.11	0.37	5	638-18-6	88.78±5.36

4-Hydroxybenzoic acid	$C_7H_6O_3$	73, 225, 283	18.4	0.06	0.08	0.28	5	99-96-7	92.58±5.37
Pinic acid	$C_9H_{14}O_4$	129, 171, 241	20.5	0.09	0.11	0.37	5	61826-55-9 (Pinonic acid)	97.31±6.29
Phthalic acid	$C_8H_6O_4$	221, 295	20.9	0.07	0.09	0.31	5	88-99-3	92.45±7.45
Isophthalic acid	$\mathrm{C_8H_6O_4}$	221, 295	21.5	0.06	0.08	0.28	5	121-91-5	94.27±3.05
Terephthalic acid	$\mathrm{C_8H_6O_4}$	221, 295	22.1	0.09	0.11	0.37	5	100-21-0	95.04±6.27
3-methyl-1,2,3-butanetricarboxylic acid (MBTCA)	$C_8H_{12}O_6$	204, 245, 405	22.4	0.09	0.12	0.39	5	61826-55-9 (Pinonic acid)	97.31±6.29
Vanillic acid	$C_8H_8O_4$	73, 223, 267	23.3	0.10	0.13	0.45	5	121-34-6	85.73±4.65
Syringic acid	$C_9H_{10}O_5$	73, 233, 297	23.6	0.09	0.11	0.37	5	530-57-4	82.66 ±1.89
β-caryophyllinic acid	$C_{14}H_{22}O_4$	117, 309, 383	25.1	0.12	0.16	0.54	10	57-11-4 (Octadecanoic acid)	93.27±2.71
Dehydroabietic acid	$C_{20}H_{28}O_{2} \\$	73, 239, 250	32.2	0.08	0.10	0.33	5	1740-19-8	97.10±1.32

Table S2. Representative compounds from various emission sources and their mass fractions in SOC and SOA. The aerosol mass fractions refer specifically to those present in $PM_{2.5}$.

Sources	Representative compounds	Precursor	f_{SOC}	SD	f_{SOA}	SD	SOA/SOC	SD	References
Biogenic	2-MGA ^a , C5-alkene triols ^b , and MTLs ^c	Hemiterpenes	0.1550	0.0390	0.0630	0.0160	2.47	0.55	Kleindienst, 2007
Biogenic	$PNA^d,PA^c,MBTCA^f,and3\text{-}HGA^g$	Monoterpene	0.2300	0.1110	0.1680	0.0810	1.37	0.15	Kleindienst, 2007
Biogenic	β-caryophyllinic acid	Sesquiterpene	0.0230	0.0050	0.0109	0.0022	2.11	0.65	Kleindienst, 2007
Anthropogenic	DHOPA ^h	Toluene	0.0079	0.0027	0.0040	0.0011	1.98	0.14	Kleindienst, 2007
Anthropogenic	Phthalic acid	PAHs (Naphthalene)	0.0390	0.0084	0.0200	0.0084	1.95	0.22	Kleindienst, 2012

 a C27α and b C29αβ: 17α(H)-22,29,30-Trisnorhopane and 17(H),21(H)-30-Norhopane.

^aC27α and ^bC29αβ: 17α(H)-22,29
 ^a2-MGA: 2-methylglyceric acid.

^bC5-alkene triols: Cis-2-methy-1,3,4-trihydroxy-1-butene, 3-methyl-2,3,4-trihydroxy-1-butene, and

Trans-2-methyl-1,3,4-trihydroxy-1-butene.

^cMTLs: 2-methylthreitol and 2-methylerythritol

dPNA: Pinonic acid.
ePA: Pinic acid

228 fMBTCA: 3-Methyl-1,2,3-butanetricarboxylic acid

g3-HGA: 3-Hydroxyglutaric acid

230 hDHOPA: 2,3-Dihydroxy-4-oxopentanoic acid

References in Table S2 Kleindienst, T. E., Jaoui, M., Lewandowski, M., Offenberg, J. H., Lewis, C. W., Bhave, P. V., and Edney, E. O.: Estimates of the contributions of biogenic and anthropogenic hydrocarbons to secondary organic aerosol at a southeastern US location, Atmos. Environ., 41, 8288-8300, https://doi.org/10.1016/j.atmosenv.2007.06.045, 2007. Kleindienst, T. E., Jaoui, M., Lewandowski, M., Offenberg, J. H., and Docherty, K. S.: The formation of SOA and chemical tracer compounds from the photooxidation of naphthalene and its methyl analogs in the presence and absence of nitrogen oxides, Atmos. Chem. Phys., 12, 8711-8726 https://doi.org/10.5194/acp-12-8711-2012, 2012.

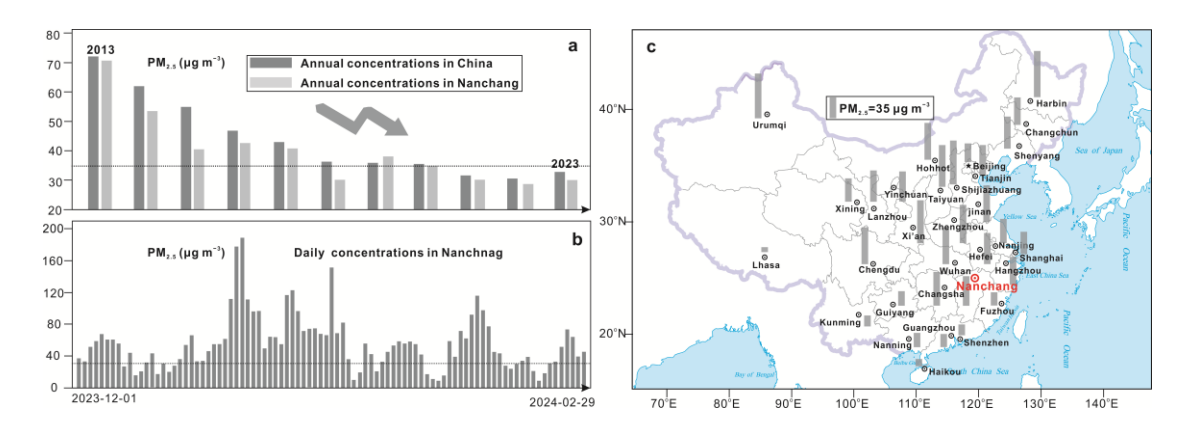


Figure S1. Trends of annual $PM_{2.5}$ concentrations from 2013 to 2023 in China and Nanchang (a); variations in daily $PM_{2.5}$ concentrations during the winter of 2023 to 2024 in Nanchang (b); winter $PM_{2.5}$ concentrations in major cities across China in 2023–2024 (c). The dashed lines in panels a and b represent the 35 μ g m⁻³ level. The base map of China in panel c is from the China Standard Map Service System (http://bzdt.ch.mnr.gov.cn). These data are from the China Air Quality Online Monitoring and Analysis Platform (https://www.aqistudy.cn/historydata/).

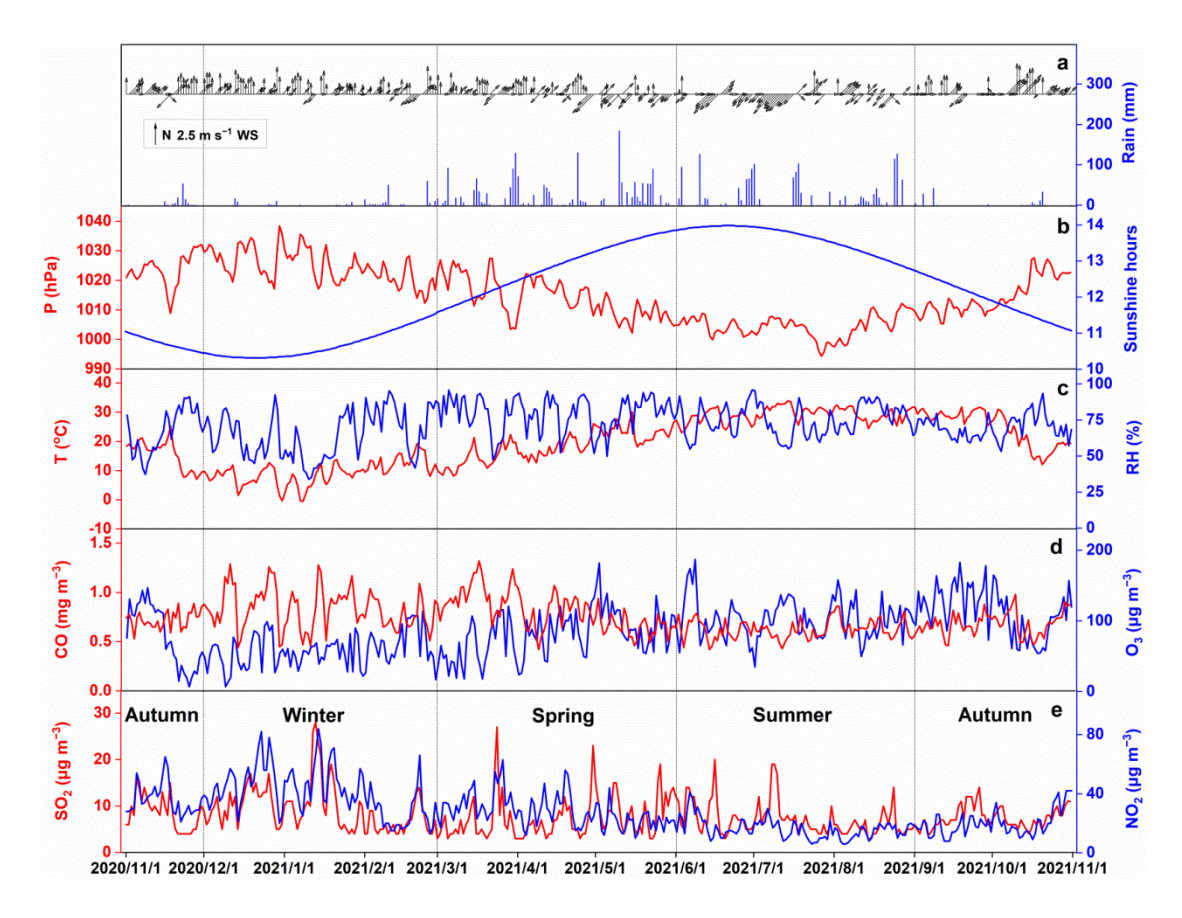


Figure S2. Time series of meteorological parameters and gaseous pollutant concentrations during sampling periods.

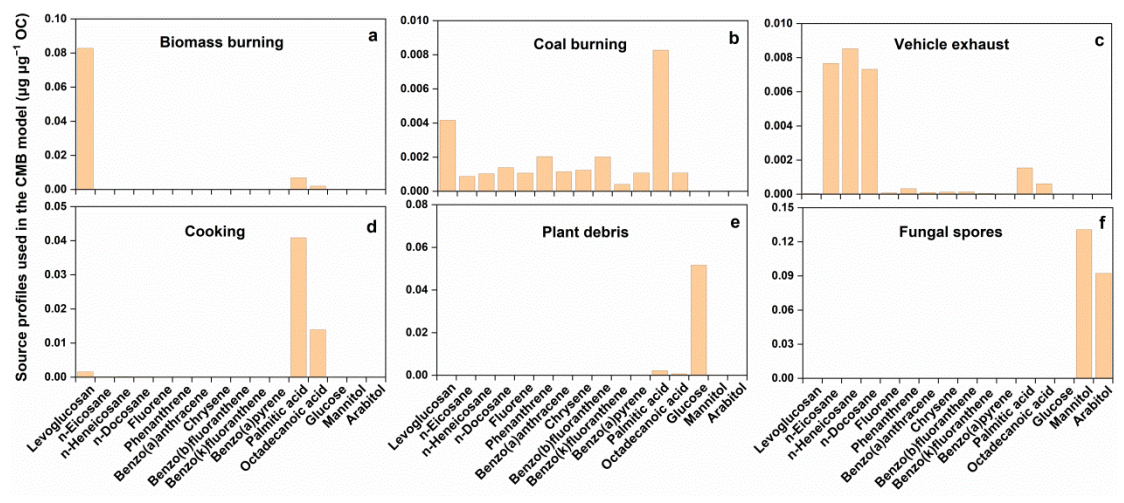


Figure S3. Source profile information used in the CMB model. Biomass burning source profile from Zhang et al. (2007); coal combustion from Zhang et al. (2008); vehicle exhaust from Cai et al. (2017); cooking from He et al. (2004), Zhao et al. (2007, 2015); plant debris from Puxbaum and Tenze-Kunit (2003); and fungal spores from Bauer et al. (2002, 2008).

- 411 References in Figure S3
- 412 Bauer, H., Claeys, M., Vermeylen, R., Schueller, E., Weinke, G., Berger, A., and Puxbaum, H.:
- 413 Arabitol and mannitol as tracers for the quantification of airborne fungal spores, Atmos.
- 414 Environ., 42, 588–593, https://doi.org/10.1016/j.atmosenv.2007.10.013, 2008.
- 415 Bauer, H., Kasper-Giebl, A., Zibuschka, F., Hitzenberger, R., Kraus, G. F., and Puxbaum, H.:
- Determination of the Carbon Content of Airborne Fungal Spores, Anal. Chem., 74, 91–95,
- 417 https://doi.org/10.1021/ac010331+, 2002.
- 418 Cai, T., Zhang, Y., Fang, D., Shang, J., Zhang, Y., and Zhang, Y.: Chinese vehicle emissions
- characteristic testing with small sample size: Results and comparison, Atmos. Pollut. Res., 8,
- 420 154–163, https://doi.org/10.1016/j.apr.2016.08.007, 2017.
- 421 He, L. Y., Hu, M., Huang, X. F., Yu, B. D., Zhang, Y. H., and Liu, D. Q.: Measurement of
- emissions of fine particulate organic matter from Chinese cooking, Atmos. Environ., 38, 6557–
- 423 6564, https://doi.org/10.1016/j.atmosenv.2004.08.034, 2004.
- 424 Puxbaum, H., and Tenze-Kunit, M.: Size distribution and seasonal variation of atmospheric
- 425 cellulose, Atmos. Environ., 37, 3693–3699, https://doi.org/10.1016/S1352-2310(03)00451-5,
- 426 2003.
- Zhang, Y. X., Shao, M., Zhang, Y.H., Zeng, L.M., He, L.Y., Zhu, B., Wei, Y.J., and Zhu, X.L.:
- 428 Source profiles of particulate organic matters emitted from cereal straw burnings, J. Environ.
- 429 Sci., 19, 167–175, https://doi.org/10.1016/S1001-0742(07)60027-8, 2007.
- Zhang, Y. X., Schauer, J. J., Zhang, Y. H., Zeng, L. M., Wei, Y. J., Liu, Y., and Shao, M.:
- Characteristics of Particulate Carbon Emissions from Real-World Chinese Coal Combustion,
- 432 Environ. Sci. Technol., 42, 5068–5073, https://doi.org/10.1021/es7022576, 2008.
- 433 Zhao, X., Hu, Q., Wang, X., Ding, X., He, Q., Zhang, Z., Shen, R., Lü, S., Liu, T., Fu, X., and
- Chen, L.: Composition profiles of organic aerosols from Chinese residential cooking: case
- study in urban Guangzhou, south China, J. Atmos. Chem., 72, 1–18,
- 436 https://doi.org/10.1007/s10874-015-9298-0, 2015.
- 437 Zhao, Y. L., Hu, M., Slanina, S., and Zhang, Y. H.: Chemical Compositions of Fine Particulate
- Organic Matter Emitted from Chinese Cooking, Environ. Sci. Technol., 41, 99-105,
- 439 https://doi.org/10.1021/es0614518, 2007.

441

442

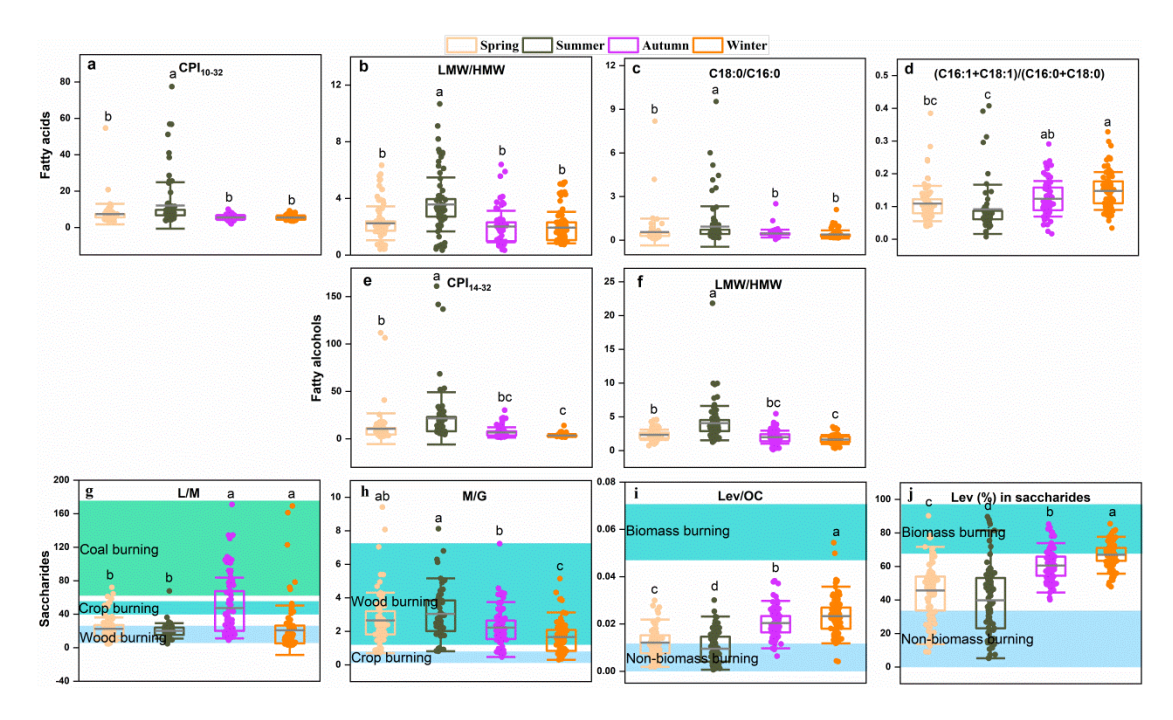


Figure S4. The concentration ratios and its seasonal variations of the major polar compounds. Each box plot illustrates the mean (centerline), interquartile range (box encompassing the 25th to 75th percentiles), and standard deviation (whiskers). The explanations for the letters a, b, c, and d on the bars are provided in the caption of Figure 2.

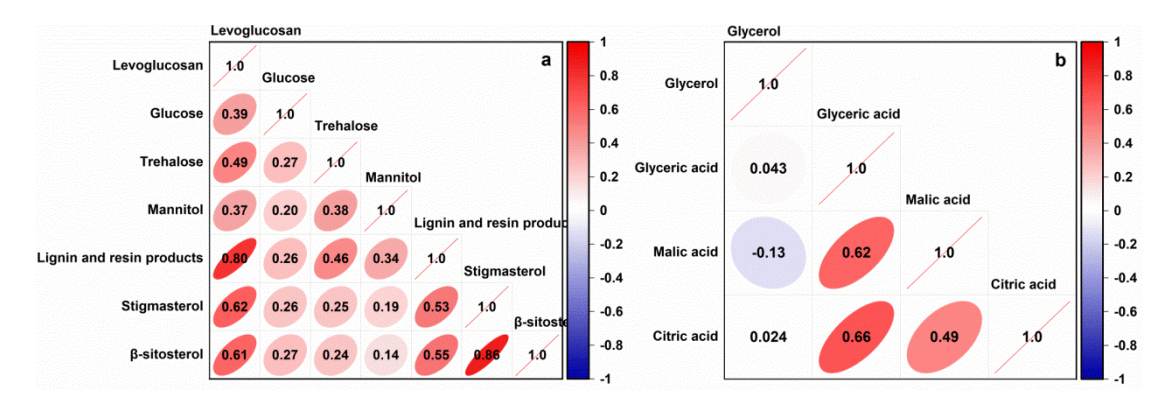


Figure S5. Correlation between levoglucosan and some primary sugars, sugar alcohols, lignin, resin products, and sterols (a); correlation between glycerol and hydroxy acids (b).

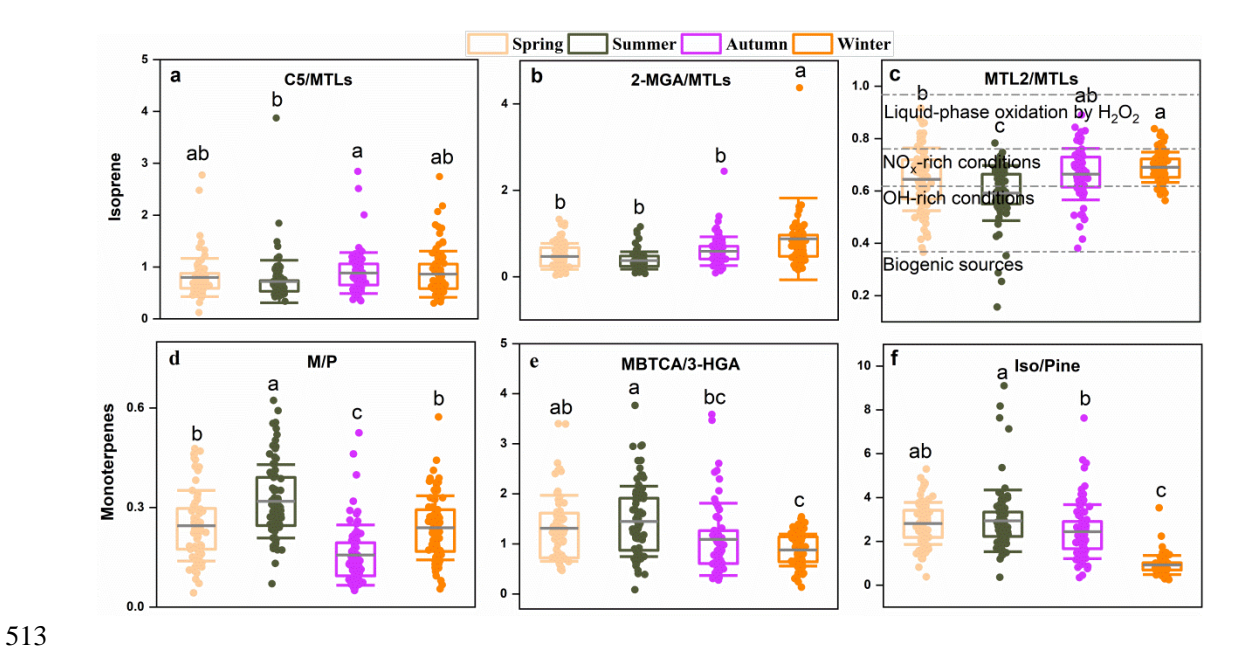


Figure S6. The concentration ratios and its seasonal variations of the SOA tracers. Box plots represent the mean (centerline), interquartile range (box encompassing the 25th to 75th percentiles), and standard deviation (whiskers). The explanations for the letters a, b, c, and d on the bars are provided in the caption of Figure 2.

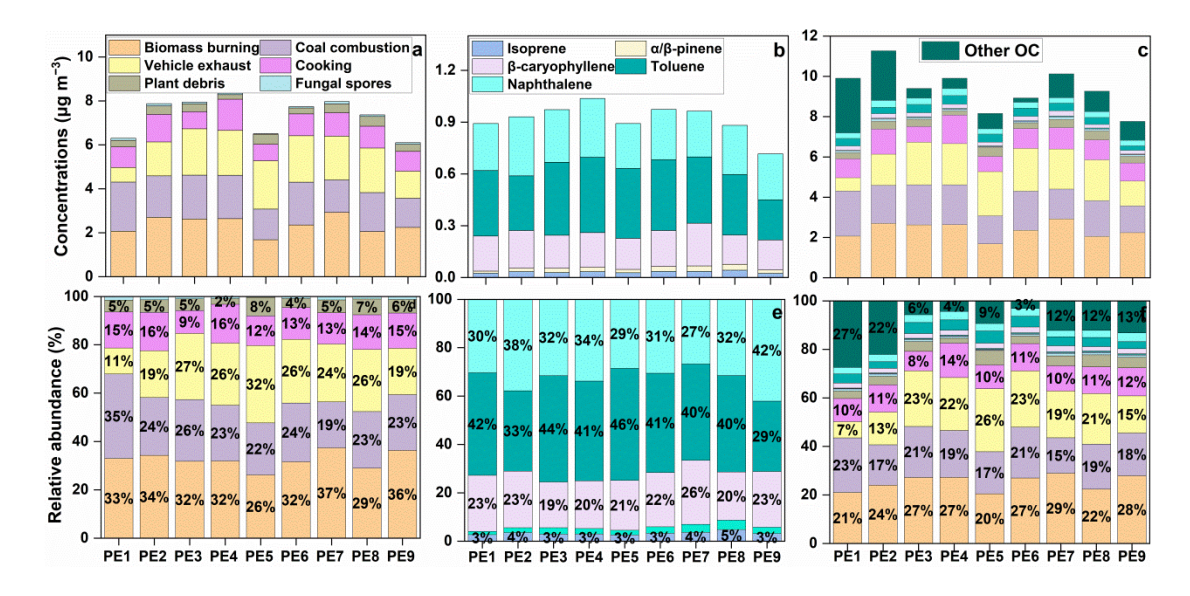


Figure S7. Concentrations and relative abundances of primary organic carbon (POC) from biomass burning, coal combustion, vehicle exhaust, cooking, plant debris, and fungal spores, as well as secondary organic carbon (SOC) from isoprene, α/β -pinene, β -caryophyllene, toluene, and naphthalene. POC and SOC concentrations were estimated using a tracer-based method, while other organic carbon (Other OC) was calculated by subtracting the estimated OC from the measured OC. PE1–PE9 correspond to winter pollution episodes 1–9.

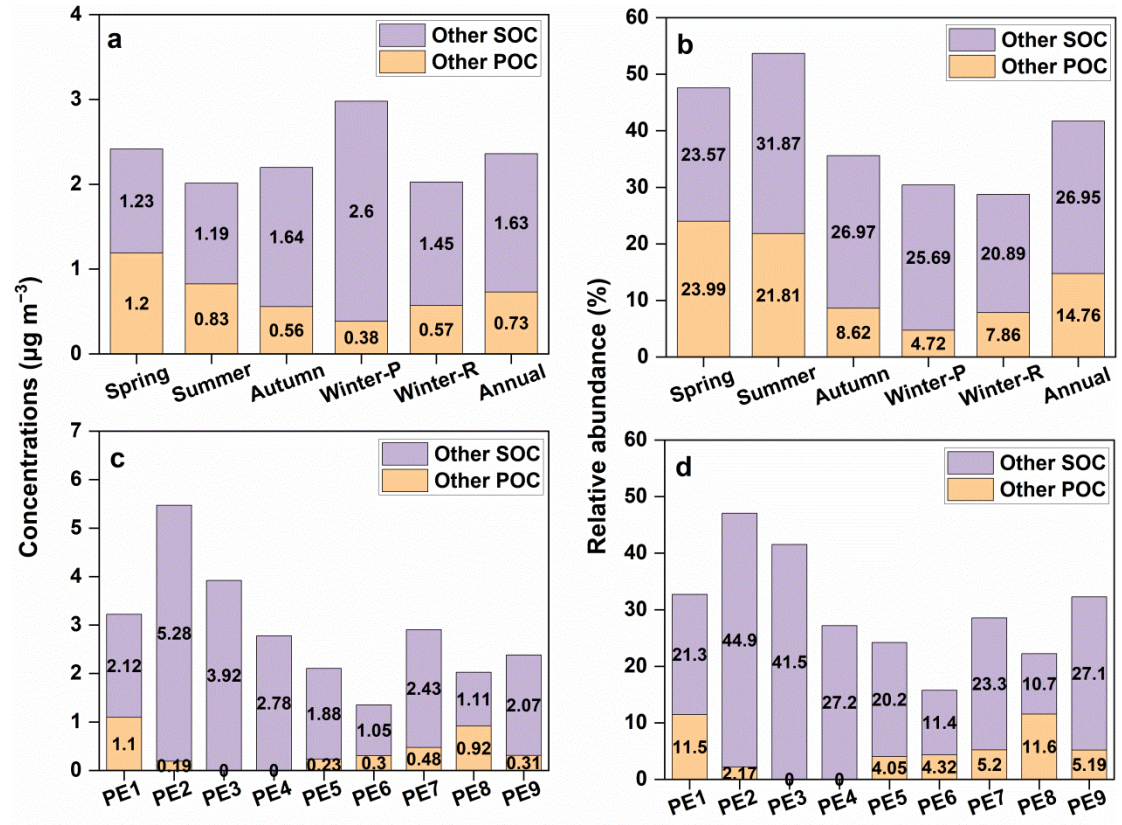


Figure S8. Variations in concentrations and relative abundances of other POC and SOC across different seasons and pollution episodes. Other POC is calculated as the difference between POC estimated by the EC-based method and POC calculated by the CMB model; other SOC is calculated as the difference between SOC estimated by the EC-based method and tracer-based SOC. PE1–PE9 correspond to winter pollution episodes 1 through 9.

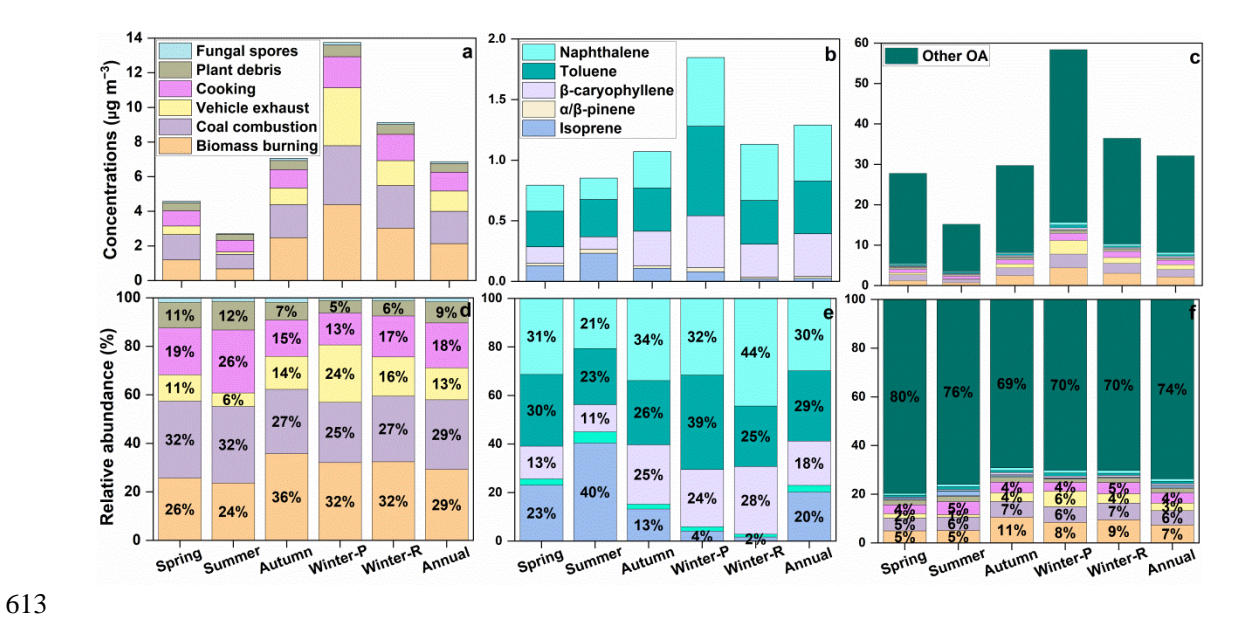


Figure S9. Concentrations and relative abundances of primary organic aerosol (POA) from biomass burning, coal combustion, vehicle exhaust, cooking, plant debris, and fungal spores, as well as secondary organic aerosol (SOA) from isoprene, α/β -pinene, β -caryophyllene, toluene, and naphthalene. Winter-P refers to winter pollution periods, and Winter-R denotes the winter remainder.

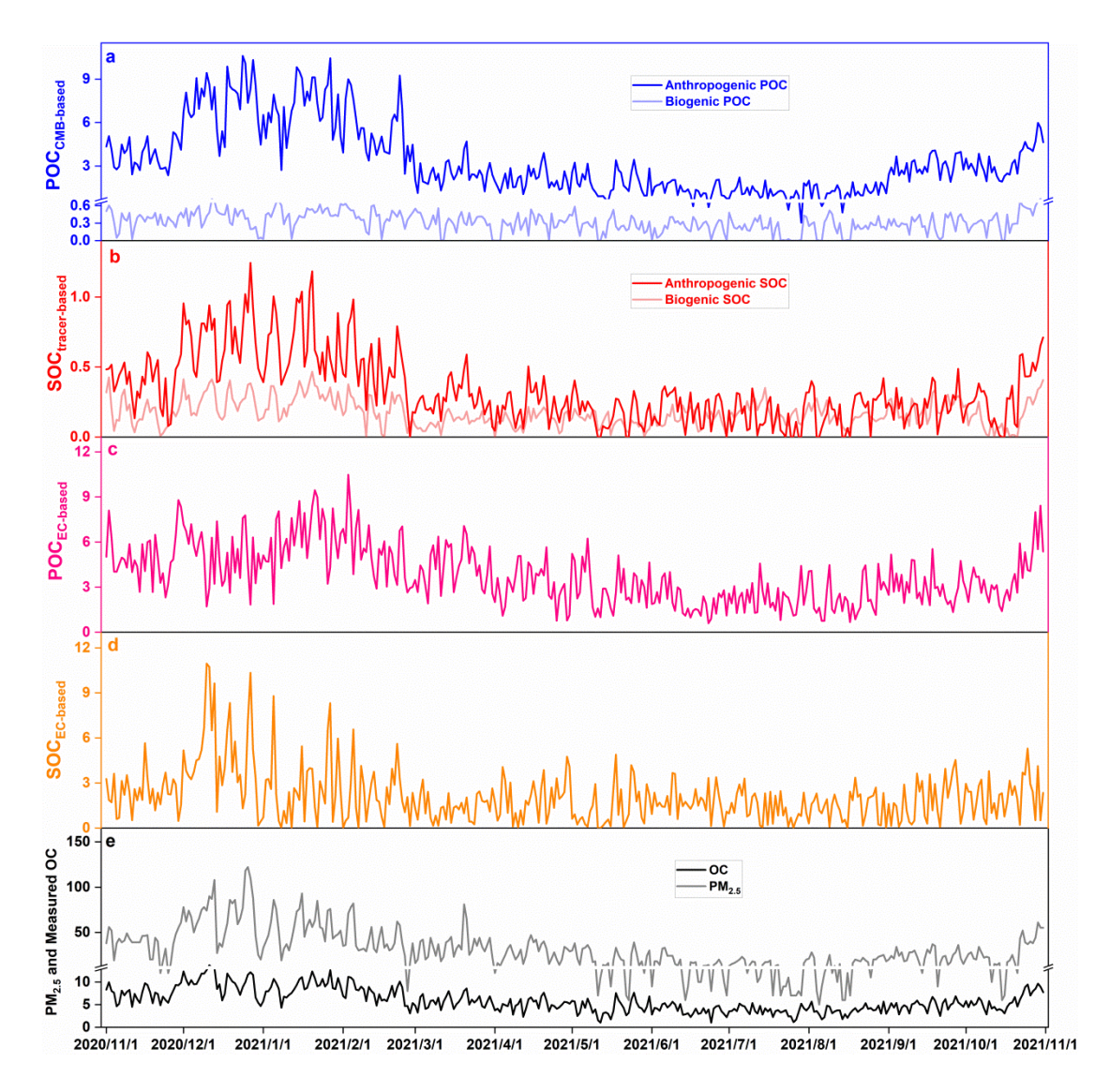


Figure S10. Time series of POC and SOC concentrations calculated using the tracer-based method, alongside POC and SOC concentrations derived from the EC-based method, as well as $PM_{2.5}$ and measured OC concentrations during the sampling period.

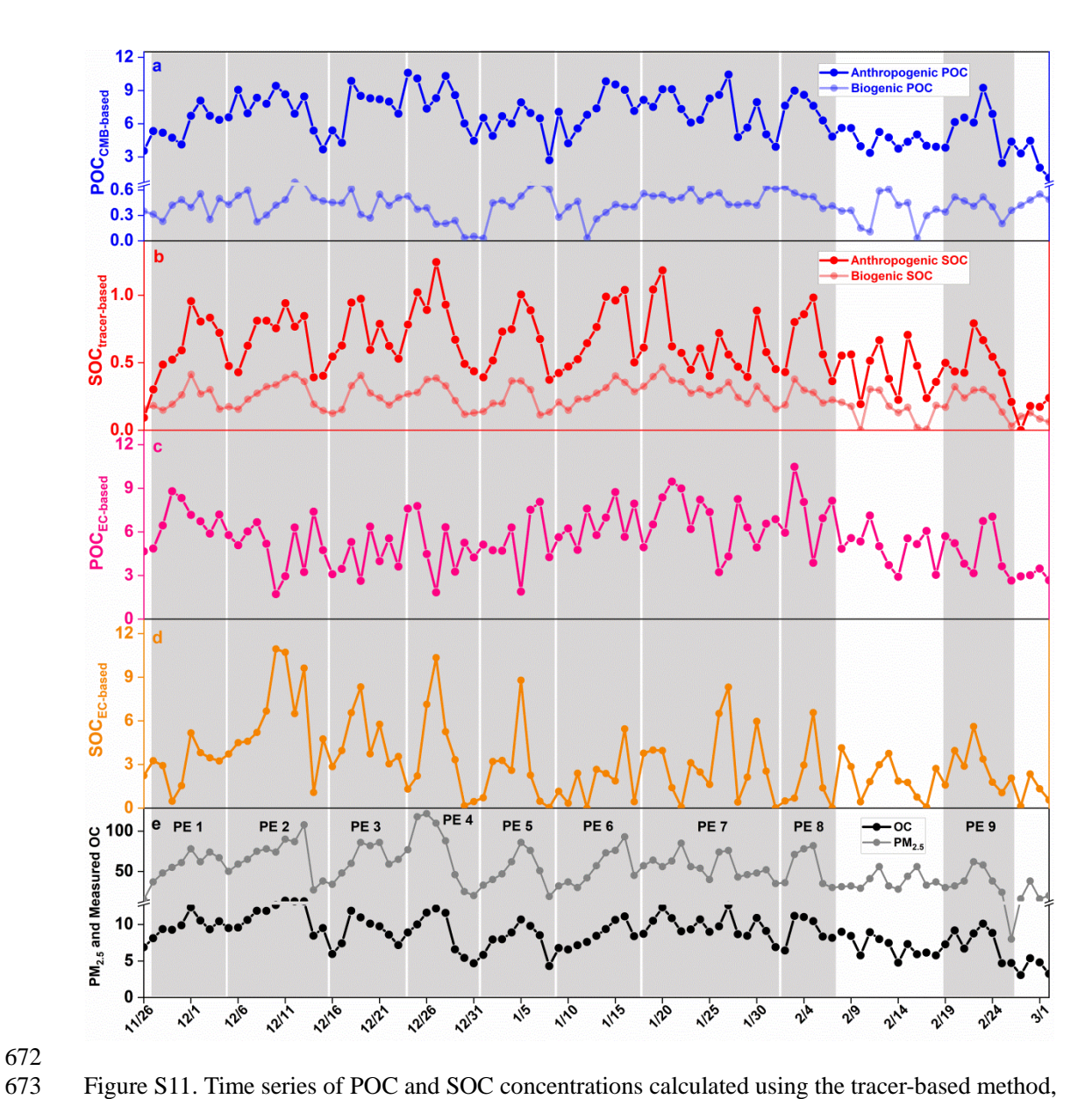


Figure S11. Time series of POC and SOC concentrations calculated using the tracer-based method, alongside POC and SOC concentrations derived from the EC-based method, as well as $PM_{2.5}$ and measured OC concentrations during winter pollution episodes.

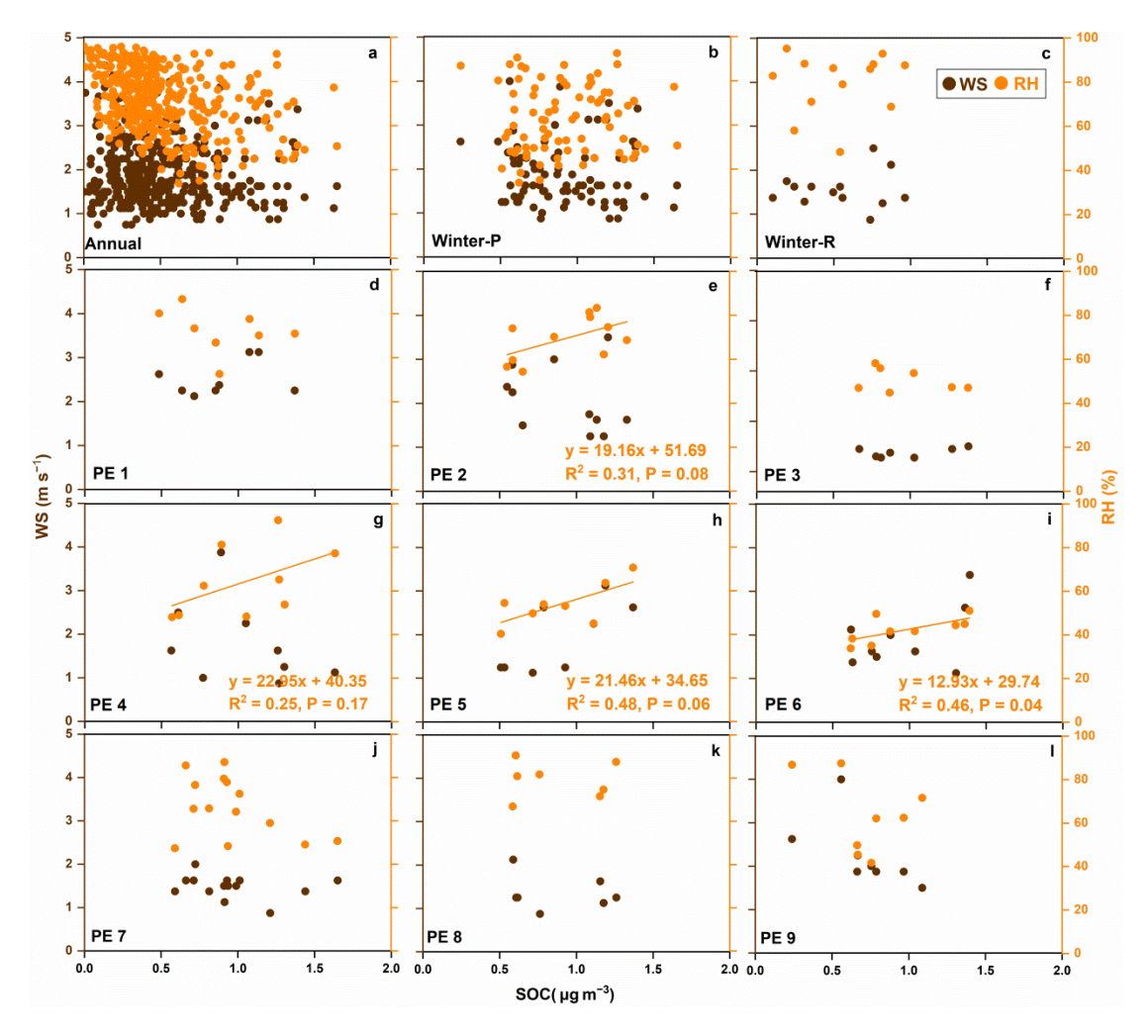


Figure S12. Linear correlation between wind speed (WS), relative humidity (RH), and SOC for the annual sampling periods (a), winter pollution periods (b), winter remainder (c), and individual winter pollution episodes (d–l). SOC concentrations were estimated using a tracer-based method. Winter-P refers to the winter pollution periods, while Winter-R denotes the winter remainder. PE1–PE9 correspond to winter pollution episodes 1–9. Before conducting linear correlation analyses, the Shapiro-Wilk test was used to assess the normality of the data, and linear correlations were conducted only for datasets significantly conforming to a normal distribution (p > 0.05).